Design of a composite tube to analyse the compressive behavior of CFRP

G. Eyer[a,*], O. Montagnier[a,b], J-P. Charles[a,c], C. Hochard[a,c]

[a] Laboratoire de Mécanique et d'Acoustique, CNRS - UPR 7051, 31 chemin Joseph Aiguier, 13402 Marseille Cedex 20, France
[b] Centre de Recherche de l'Armée de l'Air, CReA 10.401, B.A. 701, 13661 Salon-Air, France
[c] Aix Marseille Université, 60 Rue Frédéric Joliot Curie, 13013 Marseille

Abstract

A dumbbell-shaped tube is designed in order to study the compression of composites in the direction of the fibers. Three conditions are defined that ensure the validity of the experimental procedure: the cracks appear in the middle of the specimen, the strain field is homogeneous in the gauge area, and buckling must be avoided. Several tubes are manufactured and then analyzed to verify that they satisfy these three conditions. It turns out that a $[0°]_{11}$ woven carbon/epoxy (G939/M18) tube reinforced with [90°] unbalanced woven glass/epoxy tabs (1055/ES18) is suitable for compression tests.

The non linear elastic behavior of the material is then identified. The values of the parameters are close to those identified in a pure bending test.

Keywords: Compression, Experimental, Composites, Buckling, Tube, Dumbbell-shaped

Notations

Notation		Unit
t	Thickness	mm
R	Mean radius	mm
R_i	Internal radius	mm
R_e	External radius	mm
E	Homogenized modulus	MPa
ν	Homogenized Poisson coefficient	
ν_{12}	In plane Poisson coefficient	
E_{11}	Longitudinal modulus	MPa
E_{22}	Transverse modulus	MPa
E_{12}	In plane shear modulus	MPa
σ_{eq}	Equivalent stress	MPa
σ_{buckle}	Buckling stress	MPa
$\sigma_{buckle}^{corrected}$	Corrected buckling stress	MPa
ε	Strain	%
ε_c	Ultimate compressive strain	%
ε_t	Ultimate tensile strain	%
$F_{failure}$	Load leading to failure	N
N	Number of plies	
α	Non-linear parameter	

1. Introduction

Designing composite structures requires to access materials properties and to understand the mechanisms of failure for different types of load. The tests on shear and tensile strength are quite easy to do, that is why the ply properties are well identified for these types of load [1–3].

Yet in the case of compression, the experimental methods are complex and thus the knowledge of materials properties remains poor [4]. When the slenderness of the specimen is excessive in a compression test, buckling will affect the failure, but when the specimen is less slender, stress concentration generates a failure in the clamped-end. Structural effects are here the reason of the failure. It is thus not possible to conclude about the materials properties.

A solution to this problem is a compression test involving dumbbell-shaped tubes. The use of tubes permits also to impose combined load (shear/traction or shear/compression). This kind of specimen was previously used by Hochard *et al.* [5] and Miot [6]. The aim is here to describe a methodology to validate the experimental set-up in the limit case of pure compressive test. The same kind of dumbbell-shaped geometry were used for flat specimens by De Beare *et al.* [7].

First, a literature review is performed in order to identify the conditions required to validate the suitability of the test. Next, a specimen manufacturing process is presented and the experimental procedure is described. In particular, an innovative method is proposed to ensure that buckling is avoided. Finally, once the specimen has been validated, the non linear behavior and ultimate compressive stress of woven carbon/epoxy are identified.

2. Definition of a validated experimental procedure

The well-known Celanese test is advocated by the ASTM D 3410/A and EN ISO 14126 ISO norms. Due to its main advantages, i.e., the easy geometry of the sample and the classical set-up, this experimental test is often used in research [8–15]. However it gives poor strain results and failure occurs

*Corresponding Author: Gabriel Eyer, Laboratoire de Mécanique et d'Acoustique, CNRS - UPR 7051, 31 chemin Joseph Aiguier, 13402 Marseille Cedex 20, France, Tel : +33491164206

Email addresses: eyer@lma.cnrs-mrs.fr (G. Eyer), olivier.montagnier@defense.gouv.fr (O. Montagnier), jean-paul.charles@univ-amu.fr (J-P. Charles), hochard@lma.cnrs-mrs.fr (C. Hochard)

most of the time near the fixture [8, 9]. It seems to be caused by stress concentrations in this area. Moreover, there is also a risk of buckling. As a consequence, we define three conditions which have to be satisfied in order to validate a pure compressive test:

- c_1: The failure must appear in the gauge area.
- c_2: The strain field must be uniform in the gauge area.
- c_3: Failures due to buckling must be avoided.

Many research studies have thus focused on the improvement of the measurement of the ultimate compressive stress.

One way is to keep almost the same geometry and to make minor changes to the Celanese test. Lee and Soutis [8] proposed to reinforce the specimen close to the fixture and to modify the stacking sequence of plies in order to limit buckling (c_3) and stress concentration (c_1 and c_2). Unfortunately, this method does not make it possible to study a specimen in which the stacking sequence is [0°]. A second improvement [14] consists in using an âĂIJanti-bucklingâĂİ set-up to satisfy condition c_3. This method unfortunately generates friction between the anti-buckling plate and the specimen. The instrumentation of the set-up to quantify this parasitical load is a difficult and costly process.

Another way to study compression is to use a bending test and to focus on the part of the specimen submitted to compression. Bending tests are interesting as they are very stable. The main bending tests are the 3 point bending test [16, 17], the 4 point bending test [18, 19] and the pure bending test [9]. Unfortunately, some difficulties still remain:

- Condition c_2 is not satisfied and thus the relation between ultimate compressive stress and applied load necessitates to postulate about the stress state in the specimen and about the behavior of the material to solve the inverse problem [9].
- When failure is localized in the part submitted to traction, it is not possible to conclude about the failure in compression [20].
- The effects of the strain gradient on compression seem to play a part in the failure in compression [13, 21].

In the same way, Wisnom and Atkinson [21] and Drapier *et al.* [22] proposed an experimental test called âĂİconstrained bucklingâĂİ. It is a post buckling compression test on a long specimen whose ends are free to rotate. This test is thus similar to a pure bending test. The variability is low and the strain results are good.

Unfortunately bending tests do not permit to study the behavior of materials under combined load. That is the main reason to justify the choice to work with tubular specimens. The geometry of the tubes will then be defined and validated regarding the three conditions c_1, c_2 and c_3 in the case of pure compressive load.

	Carbon/Epoxy G939/M18	Glass/Epoxy 1055/ES18
E_{11} (MPa)	53000	36000
E_{22} (MPa)	53000	18000
E_{12} (MPa)	4000	4000
ν_{12}	0.035	0.19

Table 1: Elastic properties of materials used in buckling prediction

3. Materials and Sample preparation

The specimens used for these experiments are tubes. Their external diameter is set to 40 mm by the testing machine. Height is arbitrary chosen 370 mm. The manufacturing of the tubes is in two steps.

First, a tube made of woven carbon/epoxy (G939/M18 (Table 1)) is manufactured. The weave is a 4-Harness Satin. The standard designation is HTA for the fibers and M18 for the resin. The manufacturing method used is called wrap rolling [23]. It consists in rolling prepreg plies around an aluminum rod, as presented in Fig. 1. This aluminum rod is the internal mold. During rolling, a force is applied in order to compact the plies. Finally, the external ply is a heat-shrinkable tape, whose shrinking during curing ensures compaction.

For this type of resin, a curing cycle at 180°C is imposed. This method is only possible when the thermal coefficient of aluminum is greater than that of the composite. This allows the aluminum rod to be removed after the curing cycle. This method is thus particularly efficient with woven composites and works also with unbalanced composites because the thermal coefficient of the composite is significantly limited by the transverse fibers. In the case of pure UD plies oriented at 0° the method is more complex and necessitate to wind a roll of teflon around the rod in aluminum to increase the thermal coefficient of the internal mould. The internal diameter of the tube is set at 30 mm, based on the diameter of the rod. The quasi-perfect cylindricity of the rod makes it possible to consider the cylindricity defect of the tube as negligible in comparison to the classical uncertainty in the manufacturing of fibrous thermosetting composites [24]. The stacking sequence is $[0°]_n$ where n is chosen in the set {2,3,5,7,11}.

Next, the carbon tube is reinforced with tabs at both ends so that the crack occurs in the gauge area, which is the zone where the tube is not reinforced. The shape of the tube is then turned into that of a dumbbell. To obtain this shape, the number of plies is progressively increased to match the dimensions of the clamp (Figure 1). To reduce progressively the thickness, only resin epoxy with microspheres can be used. Several experiments will be performed with different materials for the tabs, such as:

- epoxy resin reinforced with microspheres,
- woven carbon plies (G939/M18),

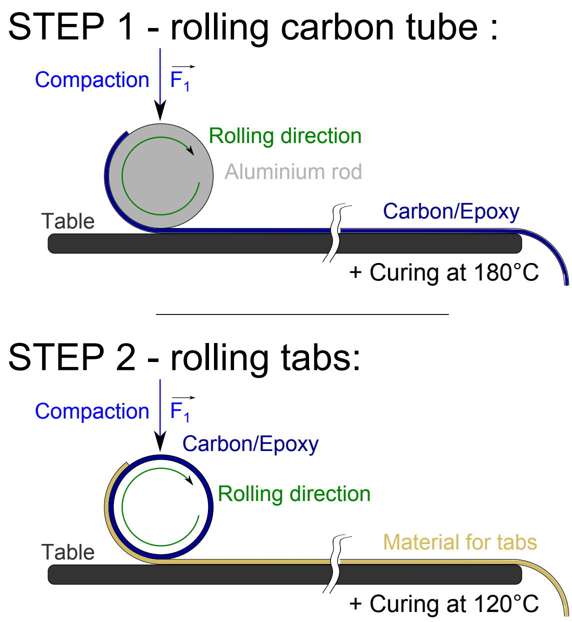

(a)

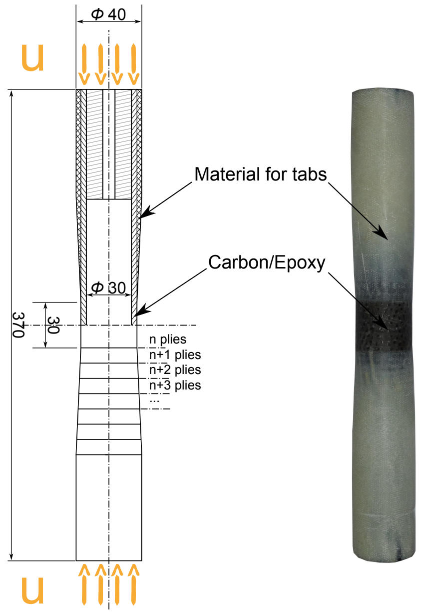

(b)

Figure 1: Manufacturing of the specimens: (a) rolling process (b) geometry of the specimen

- unbalanced woven glass [0°] plies (1055/ES18),
- unbalanced woven glass [90°] plies (1055/ES18).

The external coaxility of the tabs cannot be controlled during the curing process because the method proposed does not involve the use of an external mould. Yet, if this coaxiality is too low, bending can occur during the compressive test, which will dramatically affect the results. For this reason, the external face of the tabs is machined on a lathe. The specimen is guided internally so that the coaxiality remains satisfying.

Finally each clamped end of the specimen is filled with an aluminum rod to avoid the failure caused by machine tightening.

4. Experimental set-up and methods

A universal axial-torsion machine (MTS 322) was used for the compression test. The axial limit of the machine was 20000 daN. The uniform cross-head displacement was 1 mm/min. In order to control the homogeneity of the strain field in the specimen, the compression test was monitored by 3D Digital Image Correlation (DIC) [25]. Two cameras were needed in order to take into account the non-flatness of the specimen. The image speed was 2 images per second. This number of images per second was adapted to the monitoring of the behavior of the material during the test but it is not enough to access the mechanisms of failure. In the following sections, the validation of the test is based on the three conditions which were described in 2.

4.1. Condition c_1: The failure must appear in the strain gauge area

The specimens are dumbbell-shaped tubes, which limits the effects of the clamped ends. Yet it is observed that the choice of the material for the tabs strongly influences the localization of the crack. A post-observation makes it possible to localize the crack in each specimen. If the crack is well placed, the condition is validated. Figure 2 shows the three different areas the tube is divided in: areas A and B are zones where there is no tab, and they are thus considered as valid. Area C is not acceptable for crack occurrence.

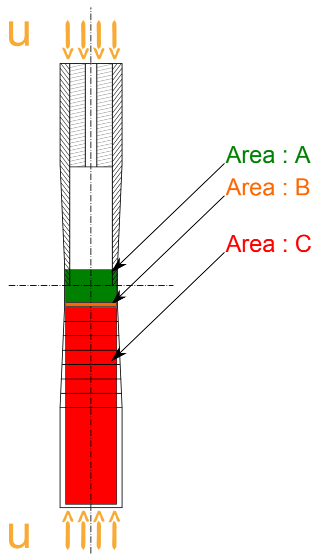

Figure 2: Definition of the area where the crack appears

Figures 3a and 3b show two post-observations of the specimen: Figure 3a (epoxy resin tab) shows that the crack has initiated in the reinforced area, while Figure 3b (woven glass at 90° reinforcement) shows that the crack is well localized in the middle of the gauge area. Table 2 shows the results for the four types of tabs. The only material unable to satisfy condition c_1 is the epoxy resin reinforced with microspheres. The presence of microspheres is necessary in order to keep manufacturing simple. Yet this additive promotes a debonding between the tabs and the carbon tube. That is why multiple cracks are observed in area C.

Material used for tabs	A	B	C
Carbon/Epoxy		✓	
Glass/Epoxy 0°	✓		
Glass/Epoxy 90°	✓		
Epoxy reinforced with microspheres			✓

Table 2: Classification of crack position vs. the material used for tabs for a 7-ply tube (areas are defined in Figure 2)

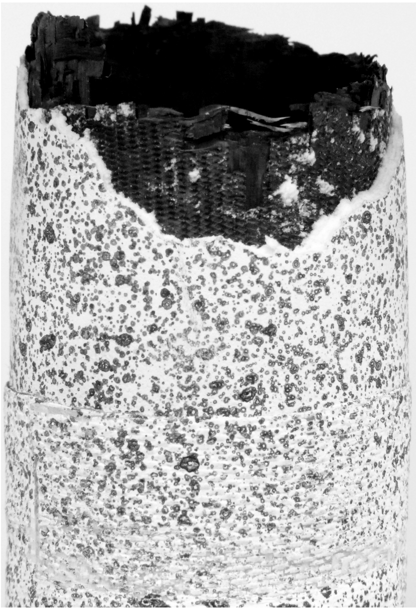

(a) Tabs made with microsphere-reinforced epoxy : crack in area C

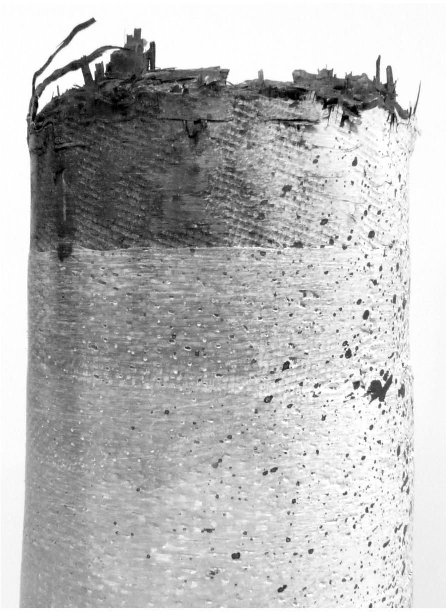

(b) Tabs made with unbalanced woven glass at 90°: crack in area A

Figure 3: Influence of the material for the tabs on the localization of the failure

4.2. *Condition c_2: The strain field must be uniform in the gauge area*

If c_2 is not validated, it is necessary to postulate on the material behavior and on the internal stress state in order to solve the inverse problem.

When this condition is validated, it is possible to calculate directly the equivalent stress state in the central gauge area, as follows:

$$\sigma_{eq} = \frac{F_{failure}}{\pi(R_e^2 - R_i^2)} \tag{1}$$

A preliminary simulation with a FE (Finite Element) model is proposed. This calculation, implemented into ABAQUS [26], takes into account the various types of tabs (Figure 4). The FE model used is a 3D shell element model, where the stacking sequence represents the different areas. Although this shell model do not permit to accurately describe the strain field in the area close to the ply drops, it makes it possible to qualitatively access the influence of the tabs on the homogeneity of the strain field in the gauge area.

This simulation shows that the softer the tabs in the longitudinal direction are, the more homogeneous the field is. In Figure 4, it can be observed that for carbon/epoxy or glass/epoxy at 0°, the strain is different in areas A and B, whereas for the other tabs the strain gradient in the longitudinal direction is smaller. The strain state is constant in the whole tube when the tabs are made of epoxy reinforced with microspheres. Unfortunately this type of tabs do not comply with condition c_1. It is then demonstrated numerically that the best tab is unbalanced glass/epoxy at 90°.

4.3. *Condition c_3: Failures due to buckling must be avoided*

Concerning c_3, it appears that the literature shows that the prediction of buckling is complex [27]. Moreover, the observation of the initiation of the failure using a high-speed camera is not possible. Here, an innovative experimental method based on theoretical results [28–30] is proposed.

Firstly, when the failure is due to material collapse, the stress leading to failure is constant. In this case, the variation in the number of plies does not affect the stress leading to failure.

Secondly, when the failure is initiated by the buckling of the structure, the equivalent stress is a function of the geometry of the specimen. In the case of thin-walled circu-

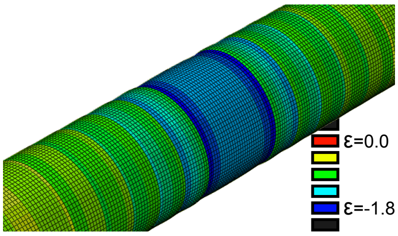

(a) Balanced Carbon/Epoxy

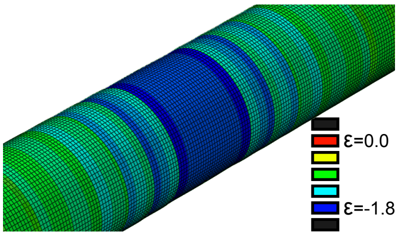

(b) Unbalanced 0° glass/epoxy

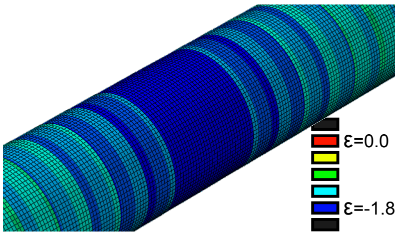

(c) Unbalanced 90° glass/epoxy

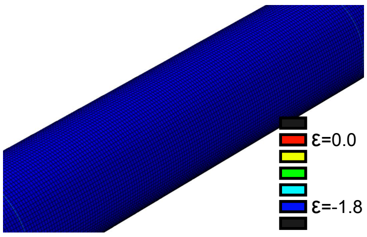

(d) Epoxy resin reinforced microspheres

Figure 4: Strain field ε_{11} for a 9 ply carbon tube and various tabs

lar cylinders and a balanced woven material, the equivalent stress can be computed using the following expression [28]:

$$\sigma_{buckle} = \frac{\sqrt{E_{11}E_{22}}}{\sqrt{3(1-\nu_{12}\nu_{21})}}\frac{t}{R} \tag{2}$$

Figure 5 is the basis of the definition of the occurrence of buckling. Various tubes with tabs made of [90°] glass/epoxy plies and with different thicknesses will be tested to identify the type of rupture. When the thickness does not modify the stress leading to failure, it will be considered that buckling does not occur. Otherwise, buckling will be supposed to be the cause of the failure. It is essential to understand here that the buckling prediction needed here to validate the experiment remains qualitative.

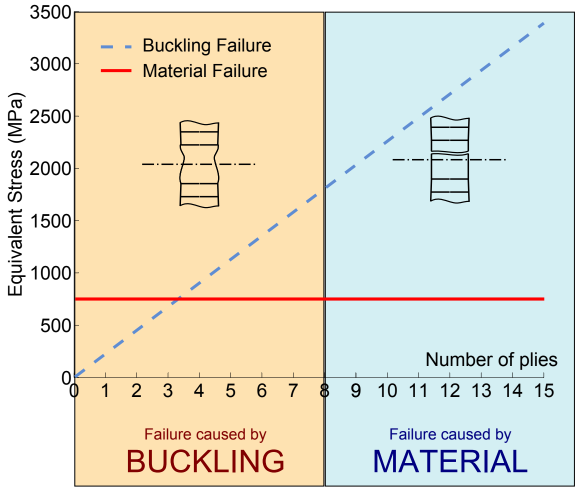

Figure 5: Theoretical prediction of the type of failure

Specimen reference	Failure load kN	Equivalent stress MPa
EC01	50	510
EC02	47	479
EC03	51	520
EC04	53	540
EC05	46	469

Table 3: Failure load for various specimens of $[0°]_3$ carbon plies

5. Experimental results and discussion

5.1. *Accuracy of the method*

First, five tests on $[0°]_3$ tubes were performed in order to quantify the accuracy of the measurement. Results are summarized in Table 3. The repeatability is good and the precision is better than 7.5 %. It will be shown later that buckling cannot be avoided in this type of tube.

5.2. *Effect of materials used for tabs*

The experimental results presented in Figure 6 confirm the numerical simulations summarized in Figure 4. The strain field is here plotted just before the collapse of the specimen. The homogeneity of the strain field is significantly affected in the ply drop area. The strain field of the tabs made of epoxy resin reinforced with microspheres is the most homogeneous because the tab rigidity is low and the variation in the tube thickness is small. Unfortunately the tubes with tabs made of epoxy reinforced with microspheres do not satisfy criterion c_1, as shown in Figure 3a.

This type of fixture is thus not appropriate. The other tabs, i.e, made of carbon/epoxy or glass/epoxy at 0° or 90° satisfy condition c_1 but an orientation with a 90° angle gives better results according to criterion c_2.

For the next experiments, tubes with tabs made of unbalanced 90° glass/epoxy will thus be used.

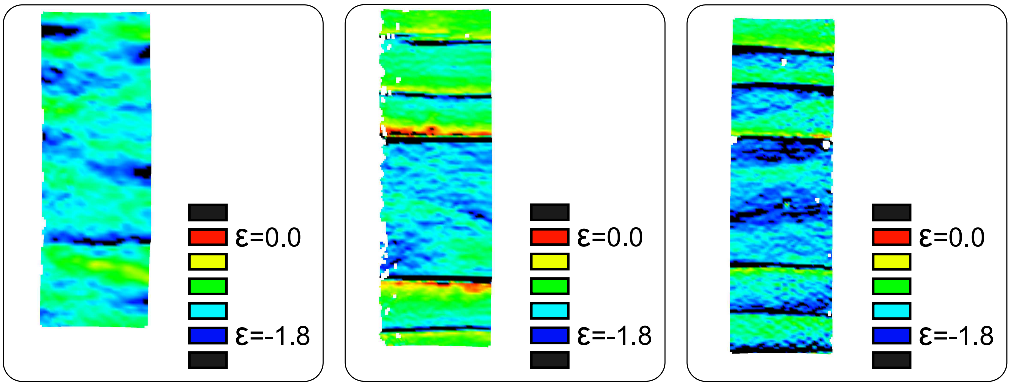

(a) Epoxy resin reinforced micro-spheres

(b) 0° glass/epoxy

(c) 90° glass/epoxy

Figure 6: Strain fields ε_{11} obtained by DIC for a 7-ply carbon internal tube with different tabs

5.3. *Choice of the number of plies*

Another issue is the choice of the number of plies. As it is shown in Figure 5, the number of plies should be sufficiently high to solve the buckling problem. But too high a number of plies implies too high a fracture load as well as manufacturing difficulties.

A validation of the specimen is proposed concerning a possible occurrence of buckling (cf. Figure 5). The compressive tests are realized for various thicknesses and the load leading to rupture is recorded for each test. The equivalent stress is next calculated using Eq. 1 and plotted in Figure 7. The thickness of the specimen is directly measured on the tube because compaction is better for a low number of plies and thus the thickness per ply can perceptibly vary.

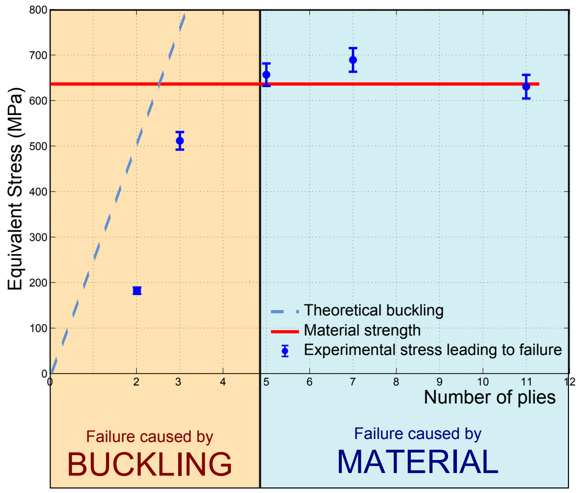

Figure 7: Results of compressive tests for various thicknesses

It is shown that the stress leading to rupture is quasi invariant when the thickness is of more than 5 plies. It is thus concluded that 7 plies will be sufficient to prevent the specimen from buckling. However, Figure 8 illustrates another issue concerning the choice between a 7-ply and an 11-ply internal tube. It is visible that the homogeneity of the strain field is better for an 11-ply internal tube. This is essentially due to the fact that the stiffness of the tab is negligible when the tube is thick. The measurement of the ultimate compressive strain will also be more accurate for this type of specimen.

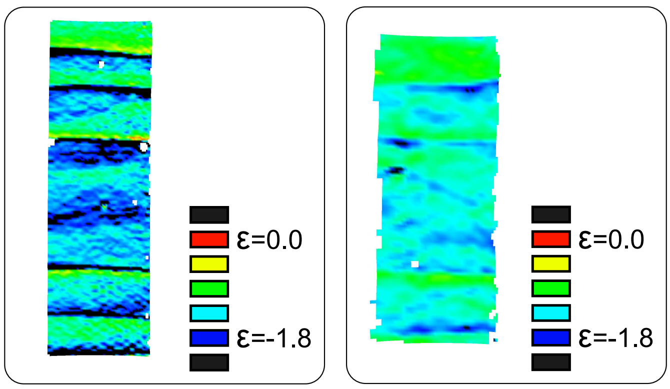

(a) 7-ply internal tube

(b) 11-ply internal tube

Figure 8: Strain fields ε_{11} obtained by DIC for a 7 and a 11-ply carbon internal tube and reinforced with a 90° glass/epoxy

For the 11-ply tube case, Figure 9 shows the evolution of the longitudinal strain around a third of the circumference of the tube (DIC field of view) for different sections in the area A. The measured strain evolves a little around the sample. This variability is associated to many parameters like the heterogeneity of the material (weaving architecture), the structure of the specimen (ply drops) and the measurement errors linked to the DIC. It is also visible that the averaged strain is quite close to the value obtained by FEM (linear model).

It should be also noted that it was researched to limit the number of overlap zones in the manufacturing process. Al-

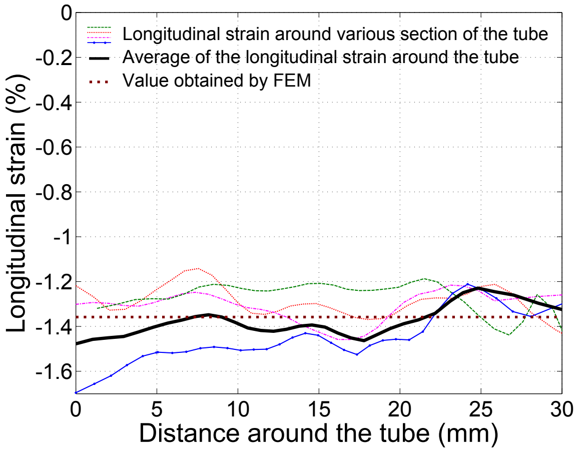

Figure 9: Longitudinal strain measured experimentally around the 11-ply tube in various sections of the area A just before collapse

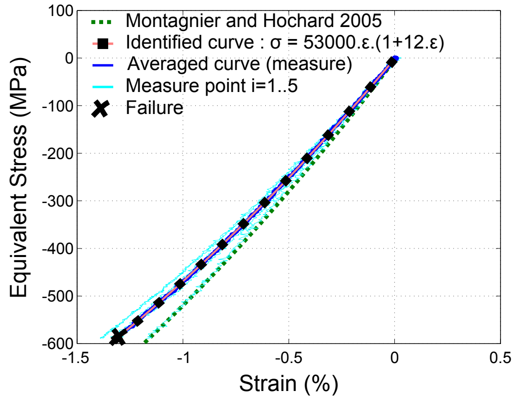

Figure 10: Non linear behavior up to failure

though it is likely that these overlap zones exist, their influence decreases when the number of plies increases. It is another reason to choose the 11-ply tube. Moreover, Figures 8b and 9 do not show sudden variations of the strain field around the circumference.

5.4. *Material behavior*

The measured strain field (Figures 8b and 9) is not perfectly uniform in the gauge area for the reasons mentioned in the previous paragraph. That is why an average strain is calculated in order to characterize the material behavior. In Figure 10, five random points were chosen to plot the σ-ε curve for a $[0°]_{11}$ tube reinforced with [90°] glass/epoxy. The average is calculated every moment by post-processing DIC results in MATLAB [31] using the following equation:

$$\varepsilon = \frac{1}{N}\sum_{i=1}^{i=N} \varepsilon_i \tag{3}$$

This strain average in the direction of the tube is ε_c =-1.35 % for the $[0]_{11}$ specimen just before collapse. This value is close to the ultimate tensile strain (ε_t = 1.5 % [32]), but the ultimate stress is different in traction and in compression because the behavior is significantly non linear in compression. This non linearity is classically attributed to the microstructure of the carbon fiber [33].

Let us identify the model proposed by Allix *et al.* [34] in order to model the non linear behavior of the material (Equation 4).

$$\sigma = E(1+\alpha\varepsilon)\varepsilon \tag{4}$$

The stiffness reduction model is in good agreement with the experimental data (Figure 10). Moreover, the values of the coefficients identified with this experiment are close to those identified with a pure bending test by Bois *et al.* [35] on a similar carbon balanced woven ply.

Concerning the failure of the composite, there is a significant difference between the pure compressive test and the bending test. The strain leading to failure with the bending test is 1.8% [35] yet the strain leading to failure is equal to 1.35% in the case of pure compressive test. This kind of results was already shown by Grandidier *et al.* [17] and Wisnom [36].

5.5. *Type of failure*

When the rupture is caused by the material collapse, the micro-buckling of the tows seems to be at the origin of the collapse of the specimen. Yet this affirmation is hard to validate because it is only based on a post-observation of the specimen. Figure 3b shows the specimen after collapse. The crack always occurs around the tube and the failure is sudden and catastrophic.

6. Conclusion

In this paper, we proposed the design of a dumbbell-shaped composite tube for pure compressive test. One of the main interest of uses tubes is the possibility to impose combined load. This kind of specimen was used in shear/traction in the past [5, 6] and in shear/compression more recently [37]. The aim is here to describe a methodology to validate the experimental set-up in the limit case of pure compressive test.

The use of tubular specimens imposes in compensation experimental difficulties that we have proposed to solve. Three conditions are then exposed in order to characterize the validity of the experiment. Solutions are then proposed for each one of these conditions:

- c_1 - *The failure must appear in gauge area:* a dumbbell-shaped tube is proposed to force the failure in the middle of the specimen.

- c_2 - *The strain field must be uniform in the gauge area:* the selection of the right material for tabs ([90°] unbalanced glass/epoxy) in order to limit the stress localization close to the ply drop zone is suggested. The use of a thick tube makes it possible to limit this stress localization.

- c_3 - *Failures due to buckling must be avoided:* an experimental procedure is developed in order to identify the occurrence of buckling. This makes it possible to determine the minimum number of plies to avoid buckling.

A $[0°]_{11}$ carbon tube with tabs made with a [90°] unbalanced glass/epoxy satisfies the three conditions defined above. In particular, the non linear behavior up to failure is well identified. The results are comparable to literature results obtained with a pure bending test, but without an inverse problem calculation. On the other hand, the strain leading to failure with the bending test is higher than in the case of pure compressive test. This is due to the gradient effect, well-known in literature.

It should be noted that the experimental measurement of compressive behavior of composites is complex. It is obviously a compromise between numerical difficulties/experimental difficulties. The approach proposed in the present paper is simple in the point of view of data reduction but complex in the point of view of experimental part. On the contrary, for constrained buckling tests or pure bending tests, the protocol is simpler but the material behavior identification is more complex.

[1] Ladeveze P, Ledantec E, Damage modelling of the elementary ply for laminated composites, Composites Science and Technology 43 (3) (1992) p.257–267.

[2] Hochard C, Payan J, Bordreuil C, A progressive first ply failure model for woven ply CFRP laminates under static and fatigue loads, International Journal of fatigue 28 (2006) p.1270–1276.

[3] Brunbauer J, Stadler H, Pinter G, Mechanical properties, fatigue damage and microstructure of carbon/epoxy laminates depending on fibre volume content, International Journal of Fatigue 70 (0) (2015) p.85–92.

[4] D. Adams, Current compression test methods, High-Performance Composites, 2005, pp. 1–7.

[5] Hochard C, Miot S, Thollon Y, Fatigue laminated composite structures with stress concentrations, Composites: Part B 65 (2014) 11–16.

[6] Miot S, Rupture de structures composites stratifiées sous chargements statique et de fatigue, Ph.D. thesis, Aix-Marseille Université (2009).

[7] De Baere I, Van Paepegem W, Hochard C, Degrieck J, On the tensionâĂŞtension fatigue behaviour of a carbon reinforced thermoplastic part II: Evaluation of a dumbbell-shaped specimen, Polymer Testing 30 (6) (2011) p.663–672.

[8] Lee J, Soutis C, A study on the compressive strength of thick carbon fibre-epoxy laminates, Composites science and technology 67 (10) (2007) p.2015–2026.

[9] Montagnier O, Hochard C, Compression Characterization of High-modulus Carbon Fibers, Journal of Composite Materials 39 (2005) p.35–49.

[10] Nafidi A, Fractography of compression failed carbon fiber reinforced plastic composite laminates, Journal of Mechanical Engineering Research 2 (1) (2010) p.1–9.

[11] Jumahat A, Soutis C, Jones F R, Hodzic A, Fracture mechanisms and failure analysis of carbon fibre/toughened epoxy composites subjected to compressive loading, Composite Structures 92 (2) (2010) p.295–305.

[12] Shokrieh M, Omidi M, Compressive response of glassâĂŞfiber reinforced polymeric composites to increasing compressive strain rates, Composite Structures 89 (4) (2009) p.517–523.

[13] Drapier S, Daridon L, Grandidier J C, Influence of some structural parameters on both theoretical and experimental compressive strength of laminates, in: International conference on composites materials, 1999, pp. 1–10.

[14] Fleck N A, Jelf P M, Curtis P T, Compressive Failure of Laminated and Woven Composites, Journal of Composites Technology and Research 17 (3) (1995) p.212–220.

[15] Guades A, Aravinthan T, Islam Md M, Characterisation of the mechanical properties of pultruded fibre-reinforced polymer tube, Materials and Design 63 (2014) p.305–315.

[16] Carbajal N, Mujika F, Determination of compressive strength of unidirectional composites by three-point bending tests, Polymer Testing 28 (2) (2009) p.150–156.

[17] Grandidier J C, Casari P, Jochum C, A fibre direction compressive failure criterion for long fibre laminates at ply scale, including stacking sequence and laminate thickness effects, Composite Structures 94 (12) (2012) p.3799–3806.

[18] Ladeveze P, Remond Y, Vittecoq E, Essais mécaniques sur composites à hautes performances : difficultés et critères de validité, Revue française de Mécanique 2 (1989) p.219–227.

[19] De Carvalho N V, Pinho S T, Robinson P, An experimental study of failure initiation and propagation in {2D} woven composites under compression, Composites Science and Technology 71 (10) (2011) p.1316–1325.

[20] Cattell M K, Kibble K A, Determination of the relationship between strength and test method for glass fibre epoxy composite coupons using Weibull analysis, Materials and Design 22 (4) (2001) p.245–250.

[21] Wisnom M R, Atkinson J W, Constrained buckling tests show increasing compressive strain to failure with increasing strain gradient, Composites Part A: Applied Science and Manufacturing 28 (11) (1997) p.959–964.

[22] Drapier S, Gardin S, Grandidier J C, Potier-Ferry M, Structure effect and microbuckling, Composites Science and Technology 56 (1996) p.861–867.

[23] Raasch, Table rolling produces durable large diameter aircraft ducts, High-Performance Composites 6 (3) (1998) p.35–X2.

[24] Mesogitis T S, Skordos A A, Long A C, Unercatinty in the manufacturing of fibrous thermosetting composites : A review, Composites : Part A 57 (2014) p.67–75.

[25] Aramis, Aramis v5. 4 user manual (2005).
URL `http://www.gom.com/metrology-systems/digital-image-correlation.html`

[26] Hibbett, Karlsson, Sorensen, ABAQUS/standard: User's Manual, Vol. 1, Hibbitt, Karlsson & Sorensen, 1998.

[27] Sosa E, Godoy A, Challenges in the computation of lower-bound buckling loads for tanks under wind pressures, Thin-Walled Structures 48 (12) (2010) p.935–945.

[28] Nemeth M P, Mikulas M M, Simple formulas and results for buckling resistance and stiffness design of compression loaded laminated-composite cylinders (2009).

[29] Eglits E, Kalnins K, Ozolins O, Experimental and numerical study on buckling of axially compressed composite cylinders, no. 10, Scientific journal of Riga Technical University. Construction Science, 2010.

[30] Hutchinson J, Knockdown factors for buckling of cylindrical and spherical shells subject to reduced biaxial membrane stress, International journal of solids and structures 47 (10) (2010) p.1443–1448.

[31] M. U. Guide, The mathworks, IEEE Signal Processing Magazine 21 (5) (2004) p.122–122.

[32] Bois C, Mesure et prévision des l'évolution des endommagements dans les composites stratifiés, Ph.D. thesis, Université d'Aix Marseille (2003).

[33] Ueda M, Saito W, Imahori R, Kanazawa D, Jeong T K, Longitudinal direct compression test of a single carbon fiber in a scanning electron microscope, Composites : Part A 67 (2014) p.96–101.

[34] Allix O, Ladevèze P, Vittecoq E, Modelling and identification of the mechanical behaviour of composite laminates in compression, Composites Science and Technology 51 (1) (1994) p.35–42.

[35] Bois C, Montagnier O, Hochard C, Caracterisation of compression be-

haviour of composite materials using a pure bending test, in: Proceedings of Journées Nationales des composites. Marseille, 2005, pp. 1–8.
[36] Wisnom M R, Size effects in the testing of fibre-composite materials, Composites science and technology 59 (1999) p.1937–1957.
[37] G. Eyer, O. Montagnier, C. Hochard, J.-P. Charles, F. Mazerolle, Effect of damage on compressive strength in fiber direction for CFRP, in: 20th International Conference on Composite Materials, Copenhagen, 2015.